



A Virtual Design Approach to Simulate the Hob Energy Performance

Daniele Landi¹ , Marta Rossi² , Claudio Favi³ , Agnese Brunzini⁴ , and Michele Germani⁵ 

¹Università Politecnica delle Marche, d.landi@univpm.it

²Università Politecnica delle Marche, m.rossi@staff.univpm.it

³Università degli Studi di Parma, claudio.favi@unipr.it

⁴Università Politecnica delle Marche, a.brunzini@pm.univpm.it

⁵Università Politecnica delle Marche, m.germani@univpm.it

Corresponding author: Daniele Landi, d.landi@univpm.it

Abstract. Eco-design strategies aim to integrate environmental considerations into product design and development. Several regulations, directives and standards have been issued on this topic during last years. In particular, European Directive (2009/125/EC) establishes the eco-design requirements related to domestic and commercial kitchen appliances (e.g. cookers, hobs, grills). The present paper focuses on the virtual product eco-design of domestic induction heating cookers, which are becoming one of the leading cooking systems due to their advantages, e.g. energy efficiency, rapid heating, cleanliness, and user safety. The adoption of numerical analysis tools for the simulation of cooktops use phase, based on thermodynamic modelling, allows to provide useful information regarding the performance of cooking system at each phase of cooking. The paper provides a progress beyond the state-of-art on thermodynamic models for induction hob simulation considering interaction between the cooktop and the pot in the work environment. The goal of the paper is therefore to propose a methodology able to support designers in evaluating heating performances of induction cooking appliances, early in the design phases, through a virtual and multi-physical product model. Thermodynamic performances are determined by measuring several parameters and reproducing the energy consumption test by the mean of a virtual prototyping tool. Results highlight how the proposed model is adherent with the real tests following a specific standard in this sector with a maximum deviation of 3.2% considering the different cooking pot sizes.

Keywords: Virtual Prototyping, Design methodology, Eco-design strategies.

DOI: <https://doi.org/10.14733/cadaps.2020.1101-1115>

1 INTRODUCTION

In last years, there was a growing interest about the environmental issue of industrial products and several regulations, directives and standards have been issued on this topic. Eco-design strategies are defined as the integration of environmental considerations into product design and development to reduce the environmental impacts of products throughout their life cycle [10]. The EU issued a specific Directive (2009/125/EC) [3] concerning the energy efficiency requirements related to household appliances, which represent the highest impacting systems after space and water heating. This Directive establishes a framework for setting mandatory ecological requirements for energy-using (EuP) and energy-related products (ErP) sold in all the EU Member States, including domestic and commercial kitchen appliances (e.g. cookers, hobs, grills). In particular, domestic induction heating cookers are becoming one of the leading cooking system due to their advantages (e.g. energy efficiency, rapid heating, cleanliness, and user safety) [25] and this cooking technology was analyzed within this work. Among the eco-design framework, the European Standard EN 60350-2 [11] regulates the measurement of energy performances for induction hobs. Product energy performance is a crucial parameter both for manufacturers and end-users. Indeed, energy performances represent a powerful marketing mainstream because efficient energy consuming products could lead to a reduction in the total amount of the consumed energy and life cycle costs. The assessment of energy performances represents a fundamental action for induction hobs manufacturers. During the last years, many researchers focused on the induction heating with different studies concerning: (i) the development of high efficiency power electronic systems, (ii) the design of the inductor, and (iii) the efficiency improvement of the cooking processes by means of the pot optimization [1], [27]. In particular, some authors studied the behavior of cooking stoves and pots with theoretical models and experiments, focusing to the thermal efficiency of pots [23]. Other researchers have analyzed the efficiency improvement of the cooking processes by means of the pot optimization, or the study of the efficiency of pots through experimental and neural network methods [22], [28]. Other works have focused on models that consider a uniform heat distribution in the bottom of the pot [2], [9]. However, these works lack in two main aspects: (i) they started from physical prototypes, and (ii) eco-design considerations are not included in the analysis. Numerical tools for the simulation of cooktops use phase, based on thermodynamic modelling, are able to provide additional information regarding the performance of cooking system. Analyzing the literature production, only few works have been developed considering thermodynamic models for induction hob simulation [13] [19].

In particular, these tools are conceived for the design and simulation of the technology, rather than for the simulation of product performances. As an example, McCarthy and Bryden [16] proposed a steady-state heat transfer model for the improvement of the cooking stoves, investigating fluids behavior around the pot. The limit of this work is that the discussion is not extended to the thermodynamic phenomena within the pot and it assumes that the water in the pot is already at the boiling temperature. Similarly, other works [8], [11] developed detailed thermodynamic model including also losses from the pot sides and heat transferred to water volume, but in both cases the water was assumed to be already at the boiling point. From the literature emerges that existing models do not consider all the parameters that are needed to allow the simulation of system operative principle under different conditions [4]. A virtual model focused on the induction hob-pot system and on its different configurations, is required to implement eco-design strategies.

The goal of the present paper is therefore to propose a methodology able to support designers in evaluating heating performances of induction cooking appliances, yet in the early design phases, through a virtual and multi-physical product model. These performances are determined by measuring several parameters in other to reproducing the energy consumption test (EN 60350-2) without to build a physical prototype. The virtual model is based on the resolution of the electromagnetic model (Maxwell equations) coupled with a thermo-fluidynamic model (mass conservation, momentum and energy conservation equations).

The paper is organized as follow: the next paragraph presents the methodological approach that leads to the evaluation of the energy efficiency of the product from the virtual model. Then the test

case used to validate the virtual model through the comparison with experimental tests is described. Finally, the conclusion section, with a discussion on the main advantages of the proposed methods and future works are presented.

2 METHODOLOGICAL APPROACH

The present research work is based on the 3D modelling (CAD system) of the system of interest (both induction system and pots) and its virtual simulation (CAE systems) using dedicated physical models (thermal and electromagnetic). Figure 1 represents the framework of the proposed approach including the adopted software tools. The virtual design approach requires the definition of three main items (i) a parametric CAD model, (ii) a multi-physical virtual model, and (iii) a real test experimental set.

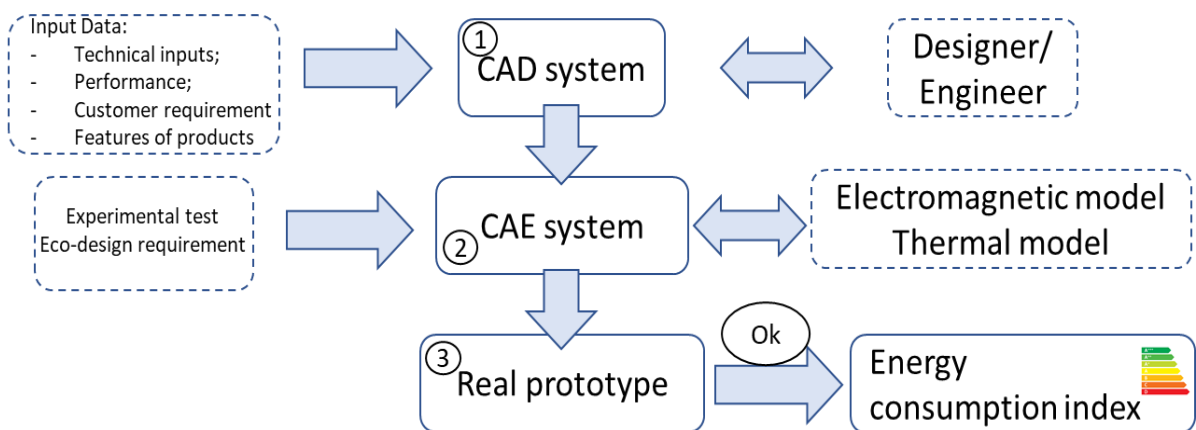


Figure 1: Methodological approach.

The approach starting with the definition of input data, such as technical inputs, performance, customer requirements, features of the product. The first phase regards the definition and the generation of a 3D CAD model. During this phase, designer and engineers develop the product virtual model of the system under analysis (Figure 2). This task is performed using mechanical 3D CAD tools. The computational effort for performing the simulations depends on the shape complexity of the CAD model.

Even the presence of a single and relatively small geometric detail (feature) can increase the size of the underlying discrete physical simulation problem by as much as 10-fold [15]. The computational time to perform a finite element analysis on a part with hundreds of small features, could be very long. Extremely large computational times may limit the usefulness of simulations during design cycles. Complex models may often lead to ill-conditioned matrices and hence working with non-simplified complex models may produce inaccurate results [21]. The use of more and more powerful processing units is not an answer to the problem associated with highly complex models. To get accurate results in a timely manner, simulations should be performed using simplified models that retain the only important details.

The resulting geometry is a model which excludes all those elements with a low influence on mechanical behavior, e.g. through holes, threads, small fillets and chambers, electrical components, etc. At this level, the main geometrical and non-geometrical parameters have to be identified and a parametric simplified CAD geometry is created.

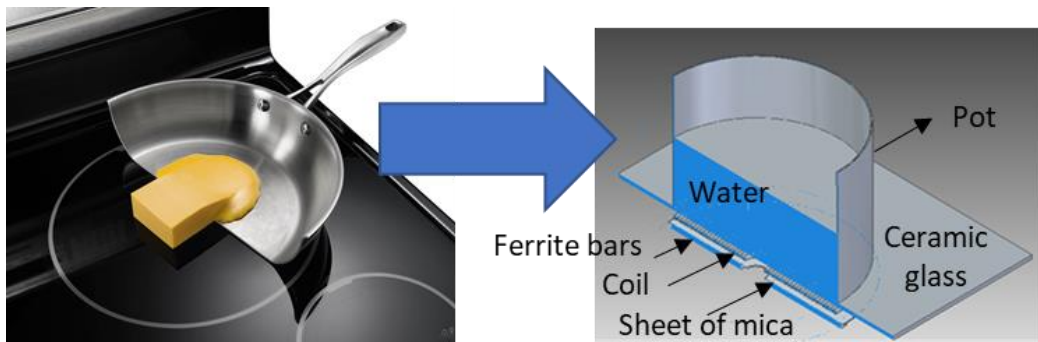


Figure 2: Parametric CAD model of induction hobs.

The second step is characterized by multi-physical model setting definition which allows to simulate the electromagnetic and thermos fluid dynamics behavior of induction hob using Finite Element Method (FEM) and Computational Fluid Dynamics (CFD) tools. The virtual prototyping level employs numerical simulation techniques to create a digital model of the product able to reproduce its behavior under certain working conditions. Currently, FEM or FVM are two of the most widely used methods to perform virtual engineering analysis. VP uses a digital model called "virtual prototype" for testing and evaluating specific characteristics of a product/manufacturing process in a computational environment. Therefore, in virtual prototyping, faults concerning fabrications, product design and production planning can be detected in a compressed time frame before great expenditures are committed. This advantage significantly reduces the number of physical iterations and thereby the associated manufacturing overheads that leads to faster and cost-effective product development. Once the virtual prototyping is created, the model may be sent directly to physical fabrication or to customers for the approval/comments. Since digital models are mostly used in VP, the cost incurred in repeating the process to optimize prototype quality is minimal. Through VP method it is possible to speed-up the design process and reduce/avoid fabrication of physical prototypes.

Independently by the adopted software tool, the simulation process is carried-out in three steps: pre-processing, processing and post-processing. During the pre-processing phase, the numerical model is built: the CAD geometry is discretized, while set up and boundary conditions are defined. The set-up phase involves defining the type of simulation (structural, fluid-dynamic, modal etc.), the principal equations of the model, and the operational conditions. The processing phase consists in the resolution of the equation defined in the previous step. The last step of VP level is the post-processing. In this phase the results obtained from the virtual simulation are collected and processed. Each physical quantity can be displayed both as a graphical trend (plane contour, vector, streamline etc.) and as a numerical table.

In this study two different models have been solved: electromagnetic and thermal models. The electromagnetic model solves the Maxwell's equations (FEM tools), calculating the eddy current phenomenon and the consequent Joule effect on the pot. The electromagnetic model used is based on the set of Maxwell equations:

$$\text{Magnetic flux equation} \quad \vec{\nabla} \cdot \vec{B} = 0 \quad (2.1)$$

$$\text{Maxwell-Gauss equation} \quad \vec{\nabla} \cdot \vec{E} = 0 \quad (2.2)$$

$$\text{Maxwell-Faraday equation} \quad \vec{\nabla} \times \vec{E} = -\frac{\partial \vec{B}}{\partial t} \quad (2.3)$$

$$\text{Maxwell-Ampere equation} \quad \vec{\nabla} \times \vec{H} = J + \frac{\partial \vec{D}}{\partial t} \quad (2.4)$$

where \vec{H} denotes the magnetic field, \vec{B} the magnetic induction, \vec{E} the electric field, \vec{D} the electric flux density, \vec{J} the electric current density associated with free charges. The following relations are for the intrinsic material properties:

$$\vec{D} = \varepsilon \vec{E} \quad (2.5)$$

$$\vec{B} = \mu_m(T, |\vec{H}|) \vec{H} \quad (2.6)$$

$$\text{Ohm law} \quad \vec{j} = \sigma(T) \vec{E} \quad (2.7)$$

where ε is the dielectric constant, μ_m the magnetic permeability, and σ the electrical conductivity. When the frequencies are low or medium, it is possible to neglect the displacement currents in the Maxwell-Ampere equation (magneto-quasi static approximation) [14].

The thermal model solves the thermodynamics equations (CFD tools). In the multi-physical model, the output obtained by the electromagnetic model is the input to the thermal one. Depending on the current and frequency that passes in the copper coil, it is possible to evaluate the eddy currents generated on the bottom of the pot and the relative heat generated by the Joule effect. The heat which is obtained through the electromagnetic model is an input to the thermal module and is able to simulate the fluid-dynamic behavior of the product.

In particular, the thermal model investigates the heat exchange and temperature distribution on the system, to determinate the energy consumption in accordance with the normative. In general, there are two methods of simulating heat, mass transfer and flow of the fluid in CFD: the first method is a single-phase method with effective physical properties such as thermal conductivity, heat capacity, density and viscosity of a composite fluid representing the characteristics of the fluid in bulk [24]. The second method is a two (or multi-) phase approach, which defines the first phase as a fluid and the second phase as a fluid cloud of particles (solid). The two-phase model is found in literature to provide improved predictions over the single-phase model [2]; as such the two-phase method with Eulerian-Eulerian approach is applied in this work. This approach assumes that at least two fluids are continuously penetrating each other. The volume fraction of the fluids in each cell sums to unity. For each fluid, the full set of conservation equations is solved. Therefore, each fluid has a different velocity field. The certain morphology of one or the other phase is neglected. This enables the limitation of computational effort to be applied for industrial problems. The information lost by averaging has to be reappear in the closure relations describing the exchange between the phases. The mechanisms of the interaction of the fluids are the momentum transfer between the phase, the mass transfer modelled by phase change and the energy transfer. Mass conservation, momentum and energy conservation equations of the multi-fluid model are represented by the following equations:

$$\frac{\partial \alpha_k \rho_k U_k}{\partial t} + \nabla(\alpha_k \rho_k U_k) = \Gamma_k \quad (2.8)$$

$$\frac{\partial \alpha_k \rho_k U_k}{\partial t} + \nabla(\alpha_k \rho_k U_k U_k) = -\alpha_k \nabla p_k + \alpha_k \rho_k g + \nabla \alpha_k (\tau^v + \tau_k^t) + U_{k,i} \Gamma_k + M_{i,k} - \Delta \alpha_k \cdot \tau_i \quad (2.9)$$

$$\frac{\partial \alpha_k \rho_k H_k}{\partial t} + \nabla(\alpha_k \rho_k H_k U_k) = -H_{ki} \Gamma_k + \alpha_k \frac{D_k}{D_t} \rho_k + \nabla \alpha_k (q^v + q_k^t) + q''_{ki} / L_s + \Phi_k \quad (2.10)$$

where the subscript k denotes the phase and i stands for the value at the interface, denotes the length scale at the interface, ρ is the density, U is the velocity vector, t is the time, p is the pressure, g is the gravitational acceleration, α is the volume fraction, τ^v is the average viscous shear stress,

τ is the turbulent shear stress) D is the interfacial shear stress, M_{i,k} is the mass generation, Γ_k the generalized interfacial drag, q''_{ki} the interfacial heat flux and Φ_k the interfacial dissipation.

The discretized conservation equations are solved iteratively until convergence. Convergence is reached when changes in solution variables from one iteration to next are negligible, overall property conservation is achieved and quantities of interest have reached steady values [5]. The accuracy of a converged solution is dependent upon: appropriateness and accuracy of physical models, assumptions made, mesh resolution and independence and numerical errors.

In terms of turbulence treatment, the dispersed phase zero equation is used for the dispersed gaseous phases, while the SST k-ω approach is used for the liquid phase. One of the advantages of the k-ω model over the k-ε is the treatment when in low Reynolds numbers for a position close to the wall. The effect of bubbles on the liquid turbulence is considered by additional source terms [20] Radiation is an existing phenomenon in the hob systems, the analysis of which via CFD has been previously carried out by Mirade et al. [17] and Mistry et al.[18]. In this study, S2S radiation models were selected. S2S radiation model's main assumption lies in neglecting all absorption, emission or scattering of radiations and considering only surface to surface radiation to be significant enough. The energy flux leaving a given surface was composed of directly emitted and reflected energy. The reflected energy flux was dependent on the incident energy flux from the surroundings, which then can be expressed in terms of the energy flux leaving all other surfaces. The energy reflected from surface K can be written as:

$$\varepsilon_K \sigma T^4 + \rho_K q_{in.K} = q_{out.K} \quad (2.11)$$

where ε the emissivity, σ is the coefficient of Stefan Boltzmann, ρ is the density, q is the energy flux and K is the surface.

The multi-physics approach requires the solution of the electromagnetic and fluid dynamic problems. The virtual modeling of the induction heating phenomenon is composed by an iterative solution of the time harmonic electromagnetic problem and the transient thermal one. In the electromagnetic analysis, FEM tool is able to estimate the heat flux in bottom of the pot, starting from the input values of current and frequency which feed the coil. The value of the heat flux of the first analysis is necessary as the input for the following thermal one with a CFD tool and for the calculation of the final output such as induction heating, temperature distribution, water heating in energy consumption test.

The last step of the methodology is the comparison between the results gained with the numerical model and the results of experimental tests performed following the dedicated standard. The aim of this comparison is to evaluate the gap between the virtual and the real models. The final result is the evaluation of the energy consumption of the product from the virtual model, since the first design phases and overcoming the need of experimental tests.

3 TEST CASE

This section presents a case study concerning the simulation of the hob energy performance. The case study involved the realization of a virtual model able to simulate the real behavior of the hob and the comparison with the experimental tests in order to validate the proposed methodology.

As describe in chapter two, the first step of the proposed approach is to define the characteristic of the hobs. In this case, a standard induction hob, which is described in Figure 3 a, has been chosen.

The output of the method is the determination of the energy consumption index in according to the European Standard. This standard (EN 60350-2:2013, [11]) defines the features to control time and temperatures during the execution of the test: the preheating period is the period of the test in which the induction plan is set to the maximum power until the water reaches a temperature of 70 [°C] (called T_c temperature in the graph). At this point, power is reduced to 25% ±5% of maximum and the water temperature still continues to rise until it reaches the temperature of 90 [°C]

(modulation period). The simmering period starts when water reaches for the first time the temperature of 90 [°C] and lasts 20 [min] in order to obtain a temperature ≥ 90 [°C]. Heating up and keeping the temperature for a defined period represent a typical household cooking process. The simmering time of 20 [min] represents an average household cooking duration (Fig. 3 (b)).

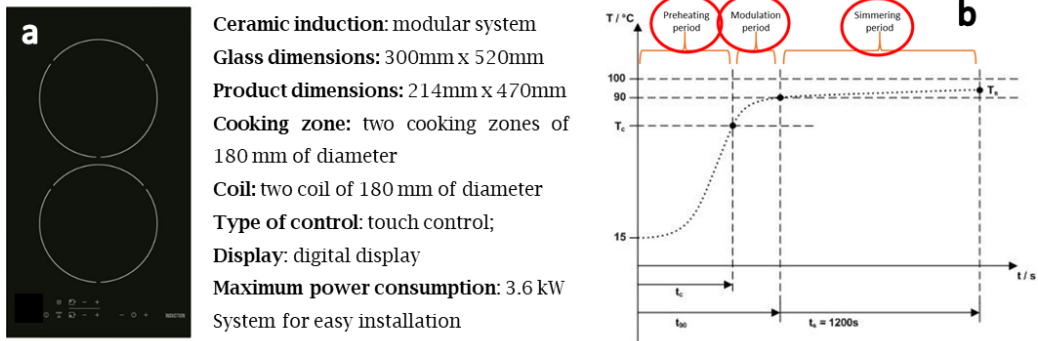


Figure 3: Induction hob data sheet (a) and eco-design test (EN 60350-2:2013) (b).

Starting from the physical characteristics of the product and the test conditions, a CAD model has been made. It is composed by: (i) a pot with lid (of different diameters 150[mm], 180[mm] and 210[mm]), (ii) a cooking surface realized in glass ceramic material, (iii) a layer of electric insulation material consisting in a sheet of mica (Potassium Aluminum Silicate), (iv) an inductor coil (180 [mm] of diameter) to generate the magnetic field, (v) a flux conveyor consisting in several ferrite bars (these latter are disposed radially and equidistant with the aim to reduce the dispersion of the magnetic field), and (vi) the water inside the pot.

For the generation of 3D CAD model, Solid-Edge® software tool by Siemens® was used. The surfaces have been made as "smoother" as possible, to allow prism layers to be extruded from the surface in the next mesh phase. Where possible, sharp angles should be replaced with radius fillets of 2 [mm]. Details smaller than a millimeter have been eliminated. Holes, threads, structural reinforcements external to case have been removed for model simplification.

As explained in the previous section, the virtual model is composed by an electromagnetic simulation and a thermal one. In order to reduce the calculation time two different CAD models have been realized in function of the physics to be solved. Figure 4 shows the difference between two models.

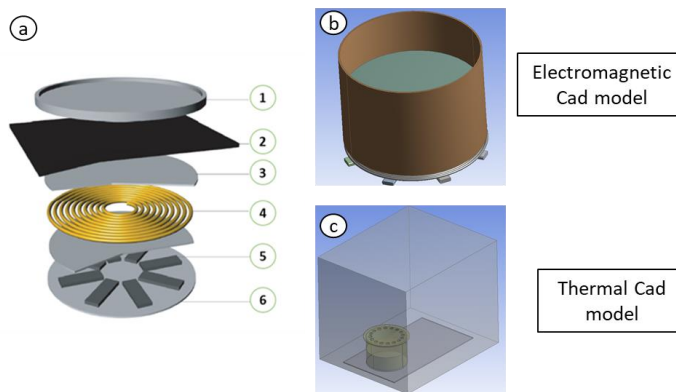


Figure 4: CAD model for the electromagnetic (b) and thermal (c) simulation.

Starting from the real model, Figure 4 (a), the two CAD models of Figure 4 (b) and (c) have been realized. The electromagnet model is composed by 8 ferrite bars, a coil of 180 [mm] of diameter, a pot with lid and the water inside the pot. All components that do not produce electromagnetic effects have been neglected, so they do not modify the results. The glass plane, pot, water and lid have been created for the thermal simulation. Moreover, the volume that represents the surrounding environment has been realized. There is no defined standard dimensions for the surrounding environment, but the volume depends by the specific case study. For each type of simulation there are best practices, deriving from the experience and know-how, which define the external environment dimensional standards. In this type of simulation, the dimensions of the external computational volume should be at least 3 pot lengths in front and behind.

In the second step of the proposed methodology, the multi physical model has been realized. The numerical simulations have been performed using commercial FEM and CFD code ANSYS® 19.0. (Maxwell® and Fluent®). A structured tetrahedral mesh was generated using ANSYS mesh. To reduce numerical diffusion during simulation, high quality mesh was created at all domains. In the development of the virtual model the parameters that can be set by the user for the simulation include: materials, pot characteristics, ambient conditions, test procedures and specific current and frequency for each power level at which the device is operated (expressed by the heat flux available at the bottom of the pot). The main outputs of the model are the trends of the water heating and the total time to complete the test in order to evaluate the energy consumption.

Standardized cookware with lid and water amount as specified in the eco-design test are used for the virtual models. The material of cookware bottom is stainless steel AISI 430 according to EN 10088-2, the thickness is 6 [mm] \pm 0,05 [mm]. The surface shall not be shiny, and the cookware is cylindrical without handles or protrusions.

The lid is made of aluminum, thickness is 2 [mm] \pm 0,05 [mm]. Each hole on the hole circle of the lid has a diameter of 16 [mm] \pm 0,1 [mm]. The holes shall be evenly distributed on the hole circle. The lid, which is flat, is adapted to accommodate a temperature sensor in the center. The temperature sensor is positioned 15 [mm] above the inner cookware bottom. The following Table 1 shows standardized cookware sizes and water amount defined in according to EN 60350-2:2013 [11].

System configuration	Diameter of the cookware bottom [mm]	Diameter of the lid [mm]	Lid hole circle diameter [mm]	Number of holes on the circle [mm]	Total cookware height [mm]	Water Load [g]
1	150 \pm 0,5	165 \pm 0,5	110 \pm 0,5	11	125 \pm 0,5	1030
2	180 \pm 0,5	200 \pm 0,5	140 \pm 0,5	16	125 \pm 0,5	1500
3	210 \pm 0,5	230 \pm 0,5	170 \pm 0,5	22	125 \pm 0,5	2050

Table 1: System specification according to EN 60350-2:2013.

For the electromagnetic simulation the input values are current and frequency on the coil. The electromagnetic solver calculates the magnetic field at the input sinusoidal frequency. The coil induces eddy currents and losses in the pot. For each system configuration of Table 1 the electromagnetic problem has been solved at different values of current and frequency. Table 2 shows the result obtain at the maximum power (preheating period) for each scenario. The values of current and frequency have been measured through physical tests.

System configuration	Network current [A]	Coil current [A]	Frequency [kHz]	Power - real [W]	Power - simulated [W]
----------------------	---------------------	------------------	-----------------	------------------	-----------------------

1	11,24	60,8	19,38	2640	2674
2	10,8	56,8	18	2500	2580
3	10,5	54,4	18,6	2353	2384

Table 2: Comparison between preheating period electromagnetic test (virtual and real test).

The same consideration has been made for the simmering period. Table 3 show the power obtain with the virtual model and during the real test.

System configuration	Network current [A]	Coil current [A]	Frequency [kHz]	Power - real [W]	Power-simulated [W]
1	1,6	15,2	49,5	368	359
2	1,7	14,6	49	391	387
3	1,75	14,7	48,5	391	380

Table 3: Comparison between simmering period electromagnetic test (virtual and real test).

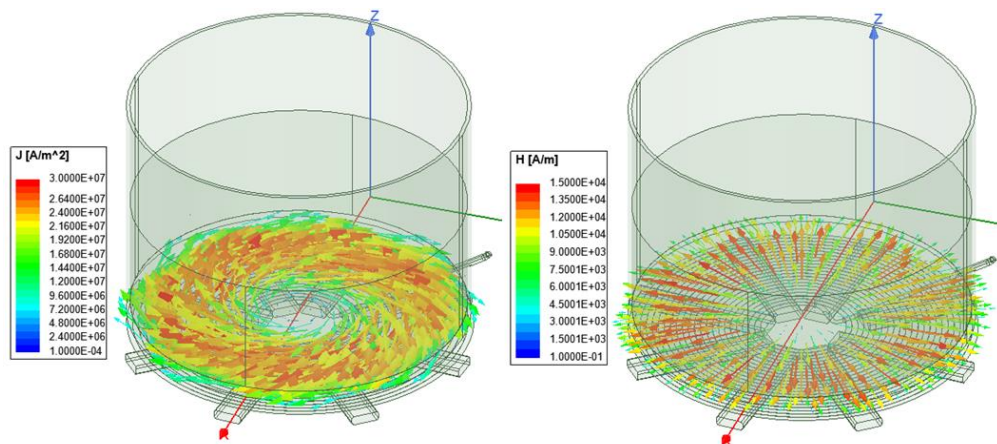


Figure 5: Trend of current the current density vector (J) and magnetic field for the 180 [mm] of pot diameter.

The solution of the electromagnetic problem converts an input of current and frequency in a power on the pot. Thanks to this model it is possible to evaluate the power transmission between the electric network and a pot, but it is not enough to determine the energy consumption index. Though use of thermal model, it is possible to analyze the behavior of the fluid inside the pot (simulating the real use of the hob) and measure the energy consumption consumed during the standard energy consumption test. The thermal simulation is composed of two steps corresponding to the "heating up period" and the "simmering period". During the simulation of the "heating up period" when the water reaches the T_c temperature, as described in the regulation EN 60350-2 - [11], the input power is reduced in order to keep the water temperature as close as possible to 90 [°C] for the "simmering period", as described by the test.

To simplify the thermal model, the following assumptions were considered: natural convection boiling, isobaric process, isothermal surface, transient condition, two phase heat transfer and

multiphase in water evaporation. Simulations were considered to solve the transient and incompressible flow, while the air fluid was considered as a perfect gas. The boundary concerns the total pressure and the ambient temperature reproduced the same required by regulation. The assumption of no-slip condition at the inside wall of the pot is valid and the convection in the pan is a laminar flow. The gravity force of $-9.8 \text{ [m/s}^2\text{]}$ is added axially in the pot. The starting temperature of the system (water, pot, glass plane) was $15 \text{ [}^\circ\text{C]}$ and the external temperature was $25 \text{ [}^\circ\text{C]}$.

Figure 6 shows the temperature trend on the middle section for the three different pots. The figure refers to end of the preheating phase (water temperature is about $90 \text{ [}^\circ\text{C]}$). From the results it is possible to note that the bottom of the pot reaches temperatures of about $170 \text{ [}^\circ\text{C]}$ and the hottest areas are the external zones. This trend depends mainly on the coil geometry. From the result of electromagnet simulation, it is possible to note a greater current density in the external areas of the bottom of the pot. This phenomenon causes non-homogeneous heating which can reduce the performance of the system.

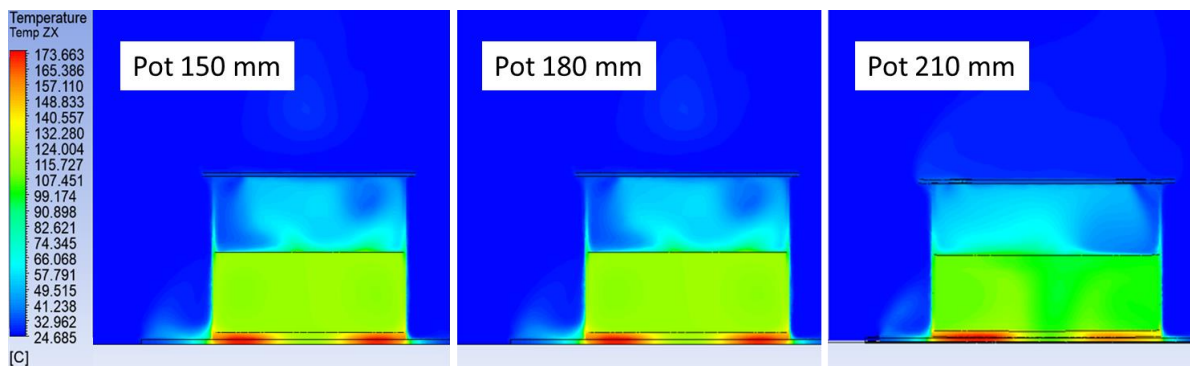


Figure 6: Trend temperature for different type of pot at the end of preheating phase.

To determine the validity of the virtual model, the comparison with experimental tests are provided. The experimental tests performed on the system comprises electromagnetic and thermal tests. The electromagnetic tests consist in the measurement of currents and frequency for each power level of the induction hob. These values are the same used as inputs in the electromagnetic virtual modelling. The measurements are obtained with a TEKTRONIK oscilloscope. All tests have been performed considering pot as a load of the system.

For the thermal test the hob and the pot are placed above a flat bench in a room with a temperature of $25 \text{ [}^\circ\text{C]}$ average. The mass of the pot and of its content was measured by means of a digital weight scale (precision $\pm 1 \text{ [g]}$) at the beginning of the test and at the end of the test. The operation allowed measuring the cumulative mass of water evaporated. A digital data logger (Delta OHM HD 9016, resolution $\pm 0.1 \text{ [}^\circ\text{C]}$), equipped with a K-type thermocouple calibrated up to $200 \text{ [}^\circ\text{C]}$, was used to measure the water temperature. The K-type thermocouple was a fine wire with $0,2 \text{ [mm]}$ diameter and was inserted into the specific hole of the lid of the pot selected for the experiments. Water temperature was thus recorded every $1,3 \text{ [s]}$ using a data logger. Ambient air relative humidity was measured by means of a digital humidity level meter (resolution $\pm 0.1\%$). Ambient air temperature was measured by means a digital thermometer (resolution $0.5 \text{ [}^\circ\text{C]}$). A wattmeter was used to read the electric power absorbed by the induction cooker at different power level and an AC/DC Current measurement system was used to read frequency and current on the coil.



Figure 7: Set up for the real test.

The following figure (Figure 8, Figure 9, and Figure 10) show the difference between real and virtual tests in function of the temperature on the pot center. For all type of pots there is a consistent correspondence between real and virtual temperature, both in the preheating and in the simmering phase.

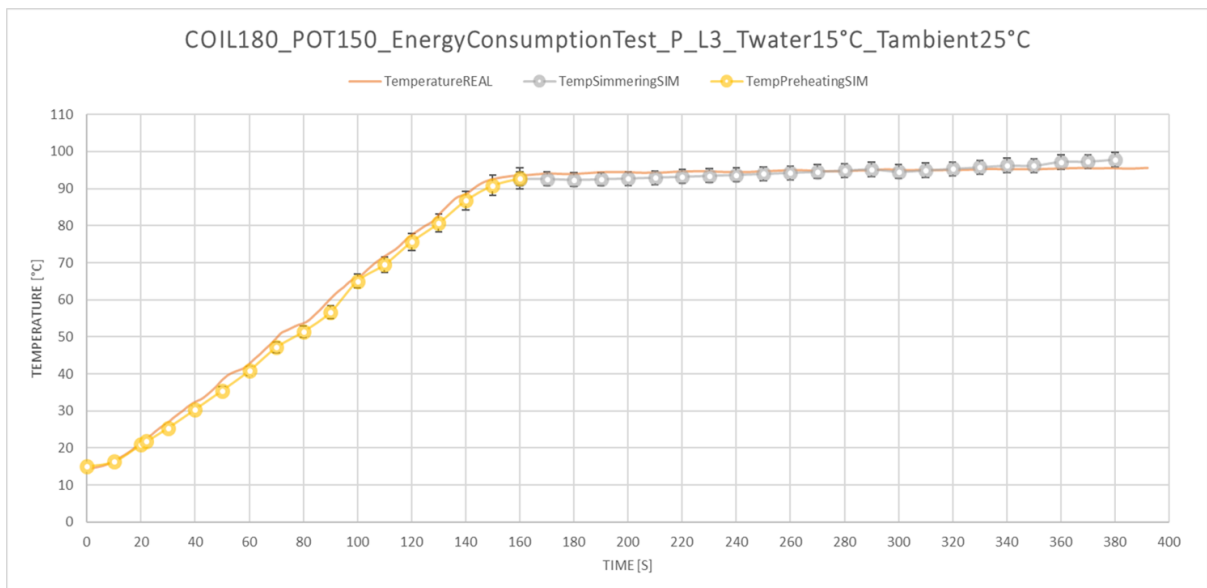


Figure 8: Comparison between real and virtual temperature for the 150 [mm] of pot.

In order to validate the whole methodology, Table 4, shows the power and energy consumption during the energy consumption test obtained with virtual and physical test. A good correspondence, both in terms of the maximum power values and the energy consumed during the test is noticed (max error = 3,2% for the 180 [mm] pot).

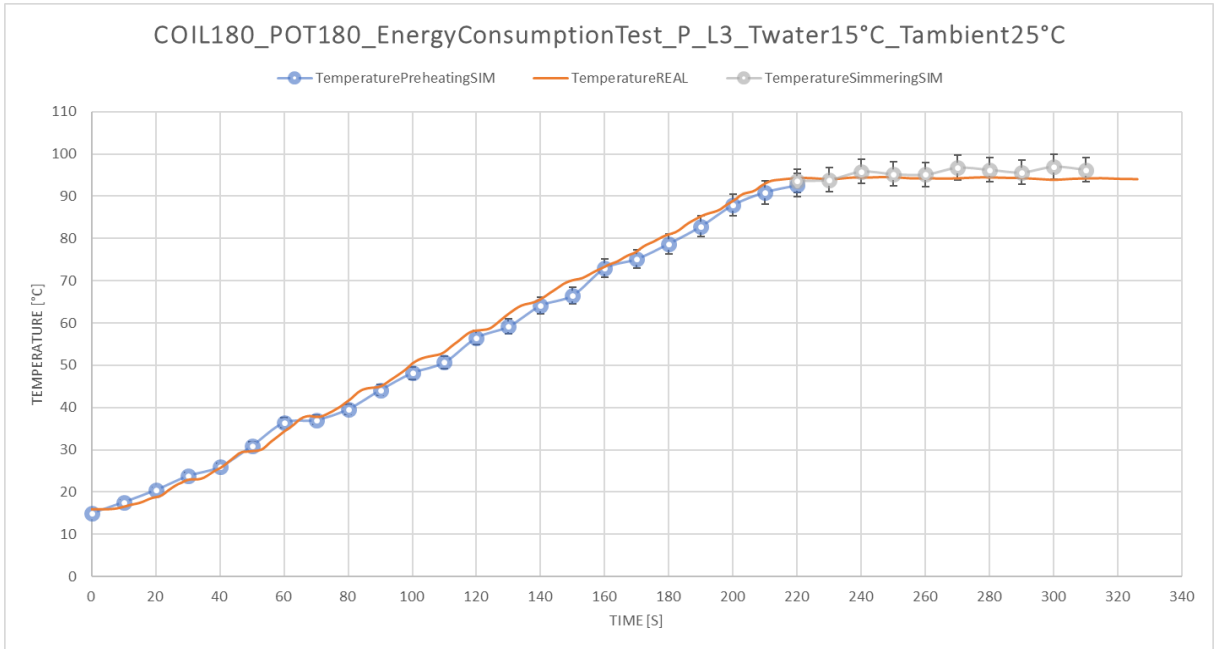


Figure 9: Comparison between real and virtual temperature for the 180 [mm] of pot.

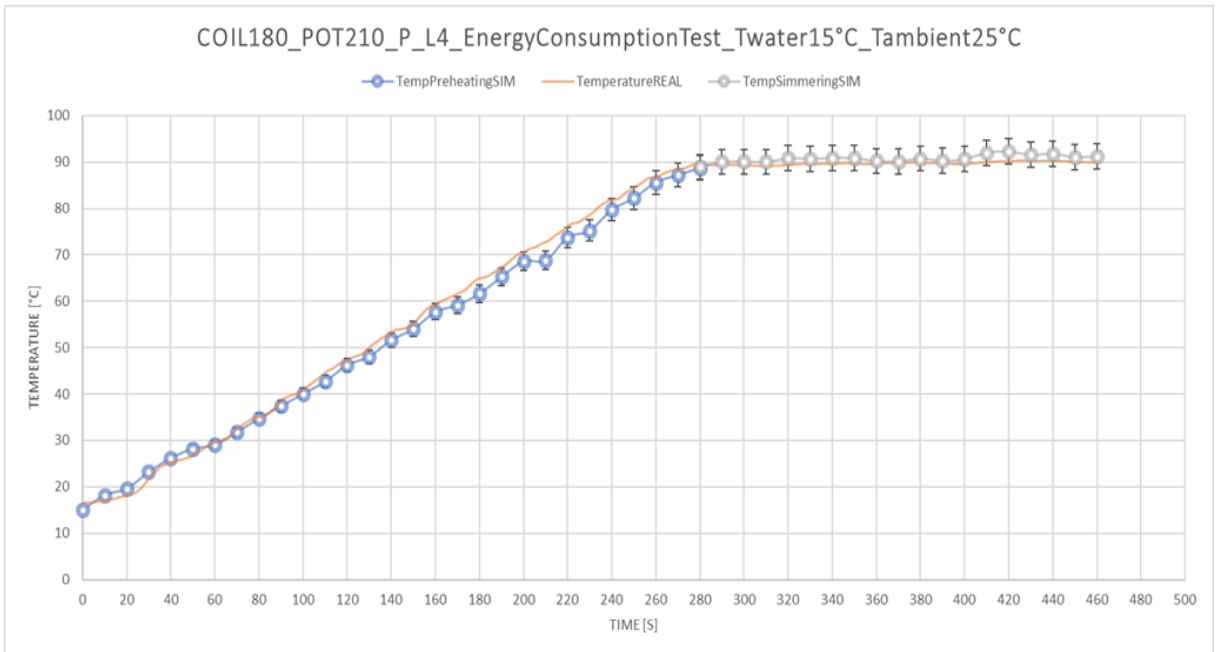


Figure 10: Comparison between real and virtual temperature for the 210 [mm] of pot.

	Pot 150 [mm]	Pot 180 [mm]	Pot 210 [mm]
--	--------------	--------------	--------------

	Virtual test	Real test	Err %	Virtual test	Real test	Err %	Virtual test	Real test	Err %
Max Power [W]	2640	2674	1.29	2500	2580	3.2	2353	2384	1.31
Energy consumption [Wh]	117.33	119.21	1.60	145.65	148.57	2.01	196.13	198.32	1.11

Table 4: Comparison between virtual and real test for 180 [mm] of coil and different type of pot.

4 CONCLUSIONS AND FUTURE DEVELOPMENT

The paper describes an approach to support designers during the design phase of household appliances. In particular, the aim of this paper is the definition of a methodological approach able to replicate, through virtual prototyping tools, the real energy consumption test, in accordance with the reference European normative.

A Multiphysics approach has been applied for the virtual analysis of both the electromagnetic behavior and the thermal fluid dynamic one. Virtual analyses (FEM and CFD) have been compared with real experiments and a gap of 3,2% has been noticed. By measuring the energy absorbed during the test of energy consumption it has been possible to quantify the energy class of the analyzed product. Through the analysis of the results, the designers can identify which are the most influential parameters on product performance and consequently make the necessary adjustments and technical considerations (eco-design actions).

The methodology proposed in the paper has been developed for induction hobs, but its structure is flexible, and it could be applied to different types of products whose operational phase is Multiphysics. Further works will consist in applying the general architecture of the proposed approach to other products, by the definition of specific models on the basis of the physical behavior to simulate.

Daniele Landi, <https://orcid.org/0000-0003-0809-3662>

Claudio Favi, <http://orcid.org/0000-0002-7176-0731>

Michele Germani, <http://orcid.org/0000-0003-1988-8620>

ACKNOWLEDGEMENTS

Authors would like to thank the Electrolux S.p.a. company and the Eng. Marcello Massaroni for the precious contribution in the development of this research.

REFERENCES

- [1] Acero, C.; Carretero, I.; Lope, R.; Alonso, O. -L.; Burdio, J.-M.: Analysis of the mutual inductance of planar-lumped inductive power transfer systems, IEEE Transactions on Industrial Electronics, 60, 2013, 410-420. <https://doi.org/10.1109/TIE.2011.2164772>
- [2] Akbari, M.; Galanis, N.; Behzadmehr, A.: Comparative analysis of single and twophase models for CFD studies of nanofluid heat transfer, International Journal Thermal Sciences, 50, 2011, 1343-1354. <https://doi.org/10.1016/j.ijthermalsci.2011.03.008>
- [3] Cadavid, F.-F. -J.; Cadavid, Y.; Amell, A.-A.; Arrieta, A.-E.; Echavarría, J.-D.: Numerical and experimental methodology to measure the thermal efficiency of pots on electrical stoves, Energy, 73, 2014, 258-263. <https://doi.org/10.1016/j.energy.2014.06.017>

- [4] Castorani, V.; Landi, D.; Germani, M.: Determination of the optimal configuration of energy recovery ventilator through virtual prototyping and doe techniques, *Procedia CIRP* 50, 2016, 52-57. <https://doi.org/10.1016/j.procir.2016.05.019>
- [5] Castorani, V.; Landi, D.; Mandolini, M.; Germani, M.: Design optimization of customizable centrifugal industrial blowers for gas turbine power plants. *Computer-Aided Design and Applications*, 16(6), 2019, 1098-1111. <https://doi.org/10.14733/cadaps.2019.1098-1111>
- [6] Delavari, V.; Hashemabadi, S.-H.: CFD simulation of heat transfer enhancement of Al₂O₃/water and Al₂O₃/ethylene glycol nanofluids in a car radiator, *Applied Thermal Engineering* 73, 2014 380–390. <https://doi.org/10.1016/j.applthermaleng.2014.07.061>
- [7] European Commission: Directive 2009/125/EC of the European Parliament and of the council of 21 October 2009 establishing a framework for the setting of ecodesign requirements for energy-related products.
- [8] Gogoi, B.; Baruah, D.-C.: Steady state heat transfer modeling of solid fuel biomass stove: part 1, *Energy*, 97, 2016, 283-295. <https://doi.org/10.1016/j.energy.2015.12.130>
- [9] Hannani, S.K.; Fardadi, M.; Jeddi, M.-K.: Mathematical modelling of cooking pots thermal efficiency using a combined experimental and neural network method, *Energy*, 31, 2006, 2969–2985. <https://doi.org/10.1016/j.energy.2005.11.006>
- [10] International Organization for Standardization (ISO), 2002. Environmental Management e Integrating Environmental Aspects into Product Design and Development, ISO 14062.
- [11] International Standard IEC 60350-2:2011, Household electric cooking appliances - Part 2: Hobs, Methods for measuring performance, Publication date 2011-12-16.
- [12] Kshirsagar, M.-P.; Kalamkar, V.-R.: A mathematical tool for predicting thermal performance of natural draft biomass cookstoves and identification of a new operational parameter, *Energy*, 93, 2015,188-201. <https://doi.org/10.1016/j.energy.2015.09.015>
- [13] Landi, D.; Cicconi, P.; Germani, M.; Russo, A.-C.: A methodological approach to support the design of induction hobs, systems, design, and complexity, *ASME International* Vol 11, 2016.
- [14] Larsson, J.: Electromagnetics from a quasistatic perspective, *American Journal of Physics* 75, 2007, 230. <https://doi.org/10.1119/1.2397095>
- [15] Lee, K.-Y.; Armstrong, C.-G.; Price, M.-A.; Lamont, J.-H.: A small feature suppression/un suppression system for preparing B-Rep models for analysis, *Proceedings of the 2005 ACM Symposium on Solid and Physical Modeling*, 2005. <https://doi.org/10.1145/1060244.1060258>
- [16] MacCarty, N-A.; Bryden, K-M.: A generalized heat-transfer model for shielded-fire household cookstoves. *Energy for Sustainable Development*, 33, 2016, 96-107. <https://doi.org/10.1016/j.esd.2016.03.003>
- [17] Mirade, P.-S.; Daudin, J.-D.; Ducept, F.; Trystram, G.; Clément, J.: Characterization and CFD modelling of air temperature and velocity profiles in an industrial biscuit baking tunnel oven, *Food Research International*, 37, 2004, 1031–1039. <https://doi.org/10.1016/j.foodres.2004.07.001>
- [18] Mistry, H.; Ganapathi, S.; Dey, S.; Bishnoi, P.; Castillo, J.-L.: Modeling of transient natural convection heat transfer in electric ovens. *Applied Thermal Engineering* 26, 2006, 2448–2456. <https://doi.org/10.1016/j.applthermaleng.2006.02.007>
- [19] Russo, A.C., Rossi, M.; Landi, D.; Germani, M.; Favi, C.: Virtual eco-design: how to use virtual prototyping to develop energy-labelling compliant products, *Procedia CIRP*, 69, 2018, 668-673. <https://doi.org/10.1016/j.procir.2017.11.076>
- [20] Rzehak, R.; Krepper, E.: CFD modeling of bubble-induced turbulence, *International Journal of Multiphase Flow* 55, 2013, 138–155. <https://doi.org/10.1016/j.ijmultiphaseflow.2013.04.007>
- [21] Saad, Y.: Iterative methods for sparse linear systems, *Society for Industrial and Applied Mathematics*, 2003.
- [22] Sanz-Serrano, F.; Sagues, C.; Llorente, S.: Inverse modeling of pan heating in domestic cookers, *Applied Thermal Engineering*, 92, 2016, 137–148. <https://doi.org/10.1016/j.applthermaleng.2015.09.084>

- [23] Shi, M.-M.: An analysis of the realization of induction cooker power control, *Journal Changshu Institute Technology*, 2, 2008, 76–78. <https://doi.org/10.4028/www.scientific.net/AMR.732-733.965>
- [24] Thakur, A.; Gopal, A.; Gupta, S.: A survey of CAD model simplification techniques for physics-based simulation applications, *Computer-Aided Design*, 41(2), 2009, 65-80. <https://doi.org/10.1016/j.cad.2008.11.009>
- [25] Villani M. G., 2011 Inchiesta su caratteristiche e utilizzo degli elettrodomestici del freddo, del lavaggio e della cottura da parte degli utenti finali, Report ENEA n. 317.
- [26] Yu, W.; Xie, H.: A review on nanofluids: preparation, stability mechanisms, and applications, *Journal of Nanomaterials*, article ID 6978130, 2018. <https://doi.org/10.1155/2018/6978130>
- [27] Zhang, C.; Zheng, Y.-J.; Sun, Z.-F.: A fuzzy control method to obtain the steady output power in induction cooker power control, *Advanced Materials Research*, 732-733, 2013, 965-971. <https://doi.org/10.4028/www.scientific.net/AMR.732-733.965>
- [28] Zorrilla, S.-E.; Singh, R.-P.: Heat transfer in double-sided cooking of meat patties considering two-dimensional geometry and radial shrinkage, *Journal of Food Engineering*, 57, 2003, 57–65. [https://doi.org/10.1016/S0260-8774\(02\)00273-X](https://doi.org/10.1016/S0260-8774(02)00273-X)